repeat the calculations for the present case, we find

$$\frac{H_c(T_N)}{H_c(T=0)}=\left[\frac{3T_N(1+\alpha)}{2(J_1+2J_2)}\right]^{1/2}, \tag{12}$$

with

$$\alpha=\frac{1}{N}\sum_{\kappa}\frac{J_1z-J_2z'(1-\mu_\kappa)}{J_1z+J_2z'(1-\mu_\kappa)}\cdot\frac{2T_N}{J_1z(1-\gamma_\kappa)+J_2z'(1-\mu_\kappa)}. \tag{13}$$

The numerical value of α is 0.68, and using Eq. (10) for J_1 and J_2, we find $H_c(T_N)/H_c(T=0)=1.1$.

ACKNOWLEDGMENTS

We wish to thank the Department of Scientific and Industrial Research for the award of a maintenance grant to one of us (A.C.H.) during the tenure of which the above research was carried out.

PHYSICAL REVIEW VOLUME 137, NUMBER 5A 1 MARCH 1965

Optical Properties and Band Structure of Wurtzite-Type Crystals and Rutile*

MANUEL CARDONA† AND GUNTHER HARBEKE‡
RCA Laboratories, Princeton, New Jersey
(Received 6 October 1964)

The fundamental reflectivity of several optically anisotropic materials (hexagonal ZnS, CdS, CdSe, and rutile) has been measured at room temperature with linearly polarized light of wavelength longer than 1100 Å. Measurements were performed with the electric vector parallel and perpendicular to the c axis of the crystal. From these reflection measurements, extended with unpolarized light to the region between 1100 and 550 Å, the optical constants have been determined by means of the Kramers-Kronig technique. The structure in the optical data of the wurtzite materials is interpreted in terms of the electronic band structure as due to direct allowed interband transitions. The interpretation is based on the existing knowledge about the related zincblende and diamond-type materials and the fact that the band structure of wurtzite along the c axis can be derived from that along the [111] axis of zincblende by applying a small hexagonal crystal field as a perturbation. The optical data on rutile reflect the ionic character of the material.

I. INTRODUCTION

THE determination of the optical constants of semiconductors at energies beyond the fundamental absorption edge by means of reflectivity and absorption measurements is a powerful way of studying the band structure of these materials.[1–5] In particular the work on cubic crystals of the diamond and zincblende structure, together with recent band-structure calculations, has provided very detailed and consistent knowledge about the position and symmetry of the electronic states involved in the direct interband transitions observed optically. A systematic correlation of all the energy gaps at critical points, i.e., points with singularities in the joint density of states of the valence and conduction bands, in the isoelectronic sequences demonstrates the similarity of the band structure of the group IV elements, III-V, II-VI, and even I-VII compounds.[5,6] Such similarity is also borne out by theoretical calculations.[7,8] Birman suggested that the band structure of the hexagonal wurtzite type crystals at points of $\mathbf{k}$ space along the hexagonal axis (c) can be derived by perturbation theory from that of the corresponding zincblende type materials along a [111] direction.[9] Hence one expects the electronic states of both types of materials to be very similar at $\mathbf{k}=0$ and along the directions just mentioned. Reflectivity measurements with unpolarized light have indeed shown that the spectra look very similar to those of the hypothetical zincblende analog as deduced from the isoelectronic sequences.[10] Also very small shifts in the position of the first absorption edge, of 0.02 eV to 0.03 eV, have been seen under different orientations of linearly polarized light with respect to the hexagonal axis of the crystals.[11–13] Moreover, the materials exhibit a very small long-wavelength birefringence.[14] Measure-

* This work was supported in part by the Advanced Research Projects Agency under Contract SD-182.
† Present address: Physics Department, Brown University, Providence, R. I.
‡ Permanent address: Laboratories RCA Ltd., Zurich, Switzerland.

[1] H. R. Philipp and E. A. Taft, Phys. Rev. **113**, 1002 (1959).
[2] M. Cardona and G. Harbeke, J. Appl. Phys. **34**, 813 (1963).
[3] J. Tauc and A. Abraham, in *Proceedings of the International Conference on Semiconductors, Prague 1960* (Czechoslovakian Academy of Sciences, Prague, 1961), p. 375.
[4] H. Ehrenreich, H. R. Philipp, and J. C. Phillips, Phys. Rev. Letters **8**, 59 (1962).
[5] M. Cardona and D. L. Greenaway, Phys. Rev. **131**, 98 (1963).
[6] M. Cardona and D. L. Greenaway, Phys. Rev. **125**, 1291 (1962).
[7] F. Herman, J. Electron. **1**, 103 (1955).
[8] F. Bassani and M. Yoshimine, Phys. Rev. **130**, 19 (1963).
[9] J. L. Birman, Phys. Rev. **115**, 1493 (1959).
[10] M. Cardona, Phys. Rev. **129**, 1068 (1963).
[11] J. A. Beun and G. J. Goldsmith, Helv. Phys. Acta **33**, 508 (1960).
[12] D. G. Thomas and J. J. Hopfield, Phys. Rev. **116**, 573 (1959).
[13] J. O. Dimmock and R. G. Wheeler, J. Appl. Phys. **32**, 2271 (1961).
[14] S. J. Czyzak, W. M. Baker, R. C. Crane, and J. B. Howe, J. Opt. Soc. Am. **47**, 240 (1957).

ments of the reflectivity spectra of wurtzite-type crystals with polarized light, however, have shown strong differences for the electric vector parallel ($E\|c$) and perpendicular ($E\perp c$) to the hexagonal axis.[15] These measurements were limited to wavelengths longer than 2100 Å. Here we report room-temperature measurements with polarized light in an extended wavelength region down to 1100 Å. The data have been used to calculate the optical constants for both polarizations by means of the Kramers-Kronig technique.

Rutile cannot be treated as a slightly perturbed cubic crystal; it crystallizes in the tetragonal structure ($C4$), with the lattice constants $a=4.49$ Å and $c=2.89$ Å, and the material is known to be strongly birefringent with values of about 2.4 for $E\perp c$ and 2.7 for $E\|c$ for the long-wavelength refractive indices.[16,17] Consequently we can expect pronounced polarization effects in the intrinsic absorption region. Again, however, the fundamental absorption edge at 3.1 eV shows a very small shift of 0.02 eV from $E\perp c$ to $E\|c$,[18] which cannot account for the birefringence and dispersion. We have studied the reflectivity of rutile with polarized light to 11 eV and with unpolarized light between 11 and 22 eV. The strong polarization effects observed, in contrast to the small effect at the absorption edge, account for the birefringence of the material. Structure due to interband transitions has been found up to the photon energy limit of our measurements (22 eV).

II. METHOD OF MEASUREMENT

The measurements below 6 eV were done with a 50-cm Bausch and Lomb grating spectrometer. At higher photon energies a 1-m Jarrell-Ash vacuum uv spectrometer was used in windowless operation. In both cases the reflectivity spectra were taken without a reference mirror. The photomultiplier detector was rotated around the sample to obtain incident and reflected intensities. The detector in the vacuum ultraviolet was a sodium-salicylate-coated photomultiplier (RCA 1P21).

The hydrogen continuum emitted by a Tanaka lamp with 60-cps ac excitation was used as a source of radiation between 2000 and 1600 Å wavelength, and between 1600 and 1000 Å the line spectra of several gases (H_2, He, Ne, A) emitted by the same source. Below 1000 Å we used the line spectrum of a hot-cathode gas tube operated with an argon pressure of 0.1 mm, a cathode-to-anode dc voltage of 100 V and 2 to 3 A current. The previously described source[5] was modified in a demountable version which is shown in Fig. 1. By removing the aluminum cathode holder, a deteriorated cathode can be easily replaced. This light source has been shown to give several intense lines between 1000 and 500 Å.

Until recently, measurements with polarized light had been limited to the region of operation of conventional polarizers. The limitation on the short wavelength side in a Glan prism with air gap is given by the absorption edge of calcite at 2100 Å. We have built transmission and reflection LiF polarizers operating in the region below 2100 Å both based on the Brewster-angle principle. The transmission polarizer consists of a stack of 8 LiF plates and can be used to about 1200 Å, the transmitted intensity becoming too small at shorter wavelengths. The intensity ratio of the light transmitted in the two principal polarization directions is about 3:1 for unpolarized incident light. The reflection polarizer (shown in Fig. 2) has the advantage of complete polarization for a single reflecting plate. It can also be used to somewhat shorter wavelengths, although for operation below 1100 Å the angle of incidence should be varied with the wavelength. Above 1100 Å such variation is not necessary because of the broad nature of the reflection minimum at the Brewster angle. The high degree of polarization is very desirable and hence, despite the small light intensity available, we have used the reflection polarizer in all the reflectivity measurements with polarized light in the vacuum uv region.

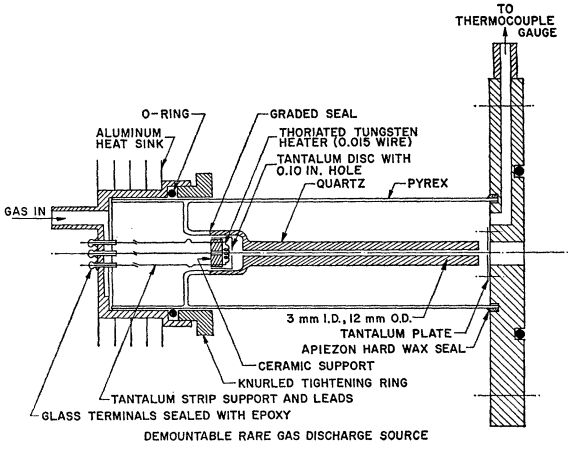

FIG. 1. Demountable hot-cathode vacuum uv source.

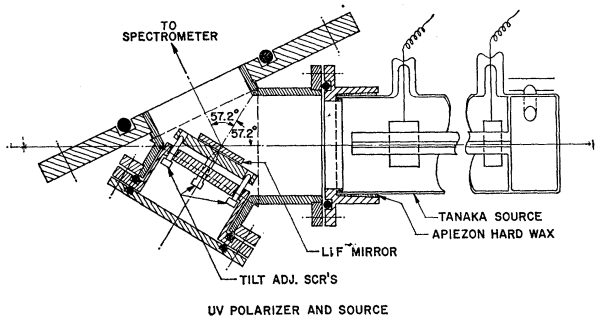

FIG. 2. Vacuum uv reflection polarizer.

[15] M. Cardona, Solid State Commun. **1**, 109 (1963).
[16] F. A. Grant, Rev. Mod. Phys. **31**, 646 (1959).
[17] J. R. Devore, J. Opt. Soc. Am. **41**, 416 (1951).
[18] P. Moch, M. Balkanski, and P. Aigrain, Compt. Rend. **251**, 1373 (1960).

All measurements at wavelengths below 1100 Å have been made with unpolarized light.

The samples of cubic and hexagonal ZnS single crystals (obtained from Semi-Elements, Inc., Saxonburg, Pennsylvania) were freshly cleaved prior to the measurements. The CdS measurements were performed on natural surfaces of platelets as grown from the vapor phase although very similar results were obtained for polished and etched ($0.5M$ $K_2Cr_2O_7$ in $16N$ H_2SO_4) surfaces. The CdSe crystals were polished in a crystal plane containing the hexagonal axis and no satisfactory etchant was found. The measurements were performed on polished, unetched surfaces and hence the spectra obtained must be somewhat smeared out. The cleaved rutile single crystals were obtained from Dr. Grabner at the National Bureau of Standards. The orientation of the c axis in all noncubic crystals was determined by x-ray diffraction.

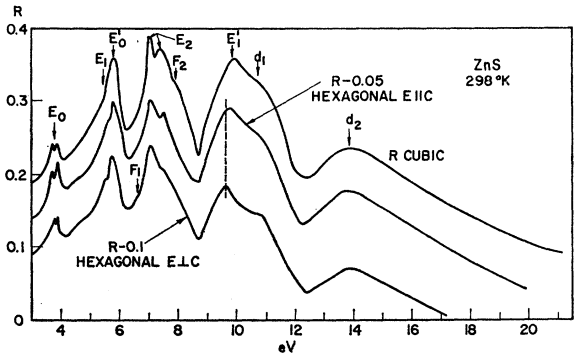

FIG. 3. Room-temperature reflectivity of cubic and hexagonal ZnS.

III. RESULTS

The room temperature reflectivity spectra of ZnS, CdS, and CdSe are shown in Figs. 3–5. ZnS provides a direct possibility of comparing the spectra of both the cubic and hexagonal modifications, the latter with light polarized parallel and perpendicular to the c axis. We notice a striking similarity in the three curves, indicating the small difference in the arrangement of the atoms in the two modifications. The assignments of the peaks labeled E_0, E_0', E_1, E_1', E_2, d_1, d_2 correspond, in the isoelectronic sequence scheme,[5,6] to peaks observed in previous work on diamond and zincblende materials. The nomenclature of the corresponding diamond and zincblende peaks has been preserved here. The subscripts 0 of E stand for transitions occurring at Γ, 1 for transitions at points in [111] direction and 2 for transitions at points in [100] direction of the $\mathbf{k}$ space in the zincblende crystal. There are some differences in the fine structure of the cubic and hexagonal ZnS spectra. The E_1 shoulder, for instance, is more pronounced for the hexagonal modification; the F_1 shoulder of the peak labeled E_2 only appears in wurtzite for $E\perp c$. The E_1'

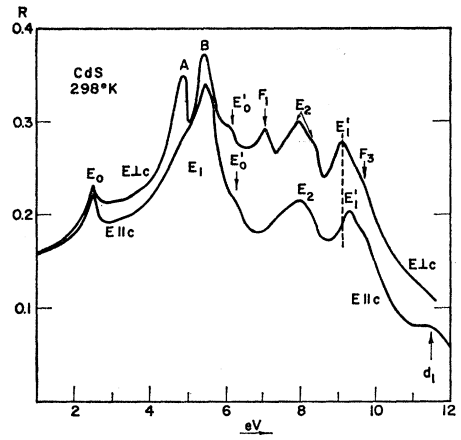

FIG. 4. Room-temperature reflectivity of hexagonal CdS for $E\perp c$ and $E\|c$.

peaks in the three spectra are slightly shifted with respect to each other, the energy of the peak for $E\|c$ being 0.12 eV higher than for $E\perp c$.

It should be noted that the ZnS spectrum is of the same type as those of C,[19] Si,[3] GaP,[4,20] and CuCl.[21] In the reflectivity spectra of materials with low average atomic numbers, the E_0' peak appears very strongly while E_1 is only a small shoulder. This situation is reversed in CdS and CdSe as in most other materials of the diamond-zincblende-wurtzite family. In these materials the E_1 peak, caused by Λ_3–Λ_1 transitions in zincblende, dominates the E_0' peak. Figures 4 and 5 show that as a result of this situation much stronger polarization effects occur. The effects around the E_1 peak have been discussed in Ref. 15. At higher energies one finds that qualitatively the same polarization features occur as in wurtzite-type ZnS, some in a more pronounced way like the F_1 peak in CdS for $E\perp c$. In all three materials F_1 appears at 0.4–0.9-eV lower energy than E_2. In CdSe there is also a weak F_1 for $E\|c$. This may be due to a breakdown in the selection

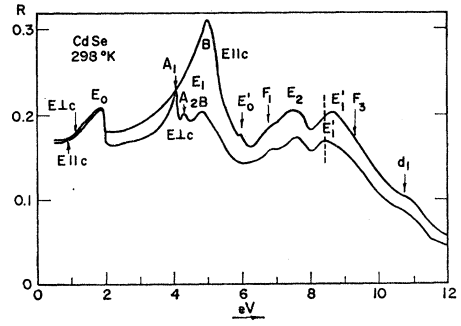

FIG. 5. Room-temperature reflectivity of hexagonal CdSe for $E\perp c$ and $E\|c$.

[19] H. R. Philipp and E. A. Taft, Phys. Rev. **127**, 159 (1962).
[20] R. Zallen and W. Paul, Phys. Rev. **134**, A1628 (1964).
[21] M. Cardona, Phys. Rev. **129**, 69 (1963).

TABLE I. Energies of the peaks in absorption index (k) and reflection (R) observed at room temperature in ZnS, CdS, and CdSe (in eV).

			ZnS		CdS		CdSe	
		Cubic	Hexagonal		Hexagonal		Hexagonal	
			$E\|\|c$	$E\perp c$	$E\|\|c$	$E\perp c$	$E\|\|c$	$E\perp c$
	R	3.66	3.74	3.78				
E_0		3.76	3.88	3.87	2.53	2.53	1.9	1.85
E_0'	k	5.82	5.86	5.80	6.2	6.1	6	
	R	5.79	5.76	5.74	6.3	6.2	6	
E_1' A	k	5.3				4.98		4.31, 4.08
	R	5.4		5.5		4.93		4.30, 4.07
B	k				5.48	5.50	4.98	4.85
	R		5.6		5.52	5.50	5.00	4.82
E_1	k	9.65	9.56	9.43	9.27	9.00	8.75	8.50
	R	9.78	9.73	9.61	9.35	9.15	8.63	8.35
E_2	k	7.03, 7.35	7.01, 7.50	7.00, 7.5	7.8	7.8	7.30	7.54
	R	6.99, 7.41	6.98, 7.56	7.00, 7.52	8.04, 8.35	8.00, 8.35	7.50	7.55
d_1	k	10.6			11.4			
	R	10.8	10.8	10.8	11.5		10.75	10.6
d_2	k	14.3						
	R	13.8	13.8	13.8	14.0	14.0	14.0	14.0
F_1	k			6.6				6.9
	R			6.6		7.12		6.8
F_2	k	7.9						
F_3	R	7.9						
					9.8	9.8	9.35	9.2

rule from a distortion of the surface by the polishing. We note again the shift in E_1' for both directions of polarization with the peak for $E\|\|c$ occurring at 0.2 eV (CdS) or 0.28 eV (CdSe) higher energy than for $E\perp c$. In Table I all the energies of the various reflection peaks in ZnS, CdS, and CdSe are compiled.

More relevant quantities for the discussion of the electronic band structure are the optical constants rather than the reflectivity spectra. We have deduced the real and imaginary parts of the refractive index n and k from the reflectivity $R(E)$ by means of the conventional Kramers-Kronig analysis. The procedure used for the extrapolation of $R(E)$ to infinite energies has been described elsewhere.[22] Figures 6 to 12 show n and k of cubic ZnS and the three wurtzite materials for $E\perp c$ and $E\|\|c$. For a comparison with the energies of the reflection peaks the corresponding values of the energies of maxima in the absorption index k are given in Table I. Figure 13 shows the near normal incidence reflectivity spectra of rutile with polarized light. The reflectivity differs for $E\perp c$ and $E\|\|c$ already at energies below the first absorption edge at 3 eV as a result of the birefringence. In the intrinsic absorption region we find an exceedingly strong dependence on the direction of polarization, in contrast to the small effect at the edge observed by transmission.[18] The dominating peak, labeled A for $E\|\|c$, seems to split into two components A_1 and A_2 having an energy difference of 1.5 eV for the perpendicular orientation. We note about the same energy difference for $E\perp c$ between B_1 and B_2, possibly

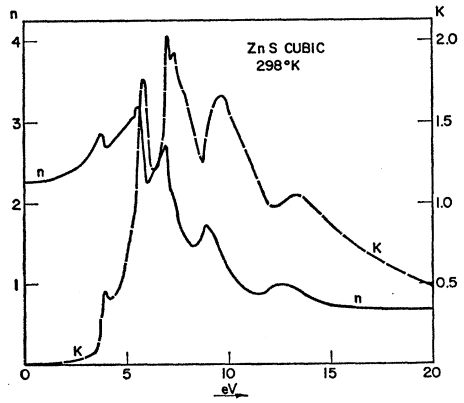

FIG. 6. Optical constants of cubic ZnS at room temperature, obtained from the Kramers-Kronig analysis of the reflection spectrum.

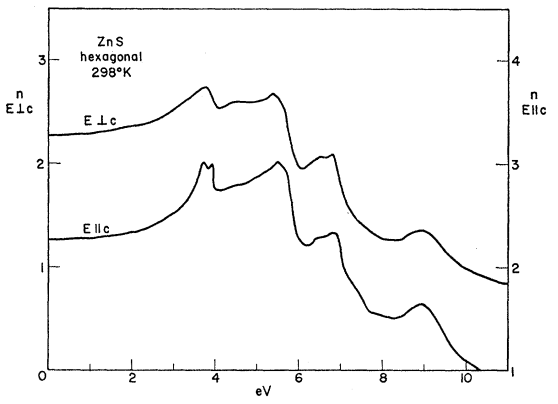

FIG. 7. Room-temperature refractive index of hexagonal ZnS for $E\perp c$ and $E\|\|c$.

[22] M. Cardona and D. L. Greenaway, Phys. Rev. **133**, A1685 (1964). Equation (5) in this reference contains a typographical error. The terms of the series expansion should be divided by $(2r+1)^2$.

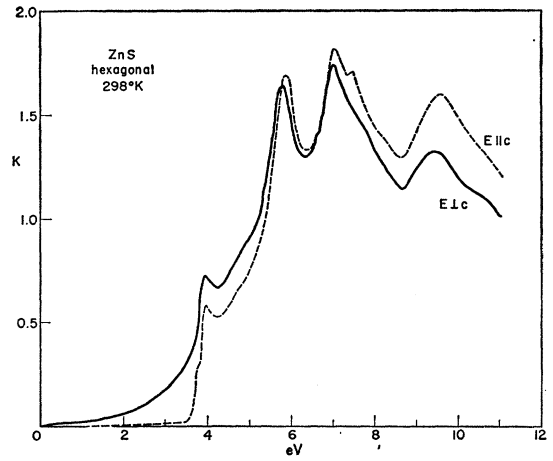

FIG. 8. Room-temperature absorption index of hexagonal ZnS for $E\perp c$ and $E\|c$.

split from the peak B observed for $E\|c$. The reflectivity at energies above the region of operation of our LiF reflection polarizer is shown in Fig. 14. The reflecting plane contained the c axis, hence our results give a

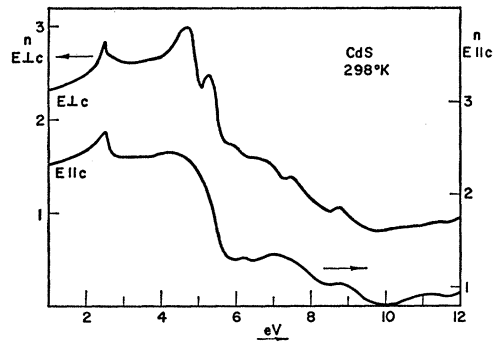

FIG. 9. Room-temperature refractive index of hexagonal CdS for $E\perp c$ and $E\|c$.

mixture of both orientations $E\|c$ and $E\perp c$. Two peaks are seen at 14.0 and 17.4 eV. The values of the various reflection peaks are given in Table II again together with the energy values of maxima in k and ϵ_2.

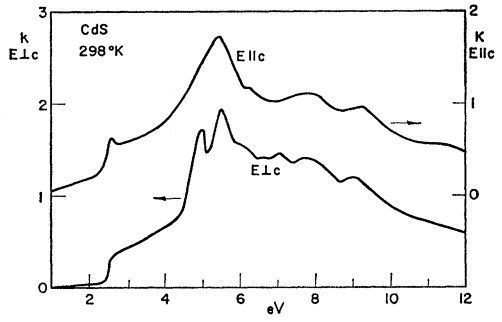

FIG. 10. Room-temperature absorption index of hexagonal CdS for $E\perp c$ and $E\|c$.

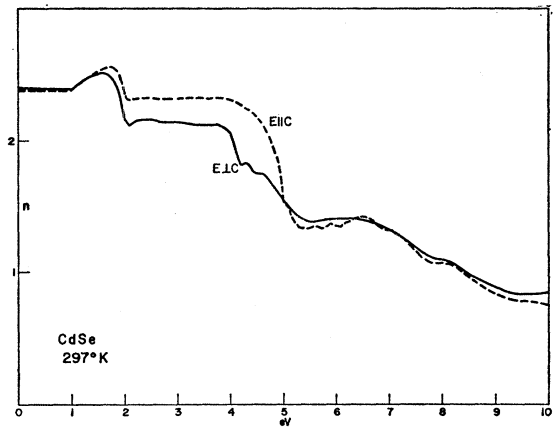

FIG. 11. Room-temperature refractive index of hexagonal CdSe for $E\perp c$ and $E\|c$.

Some problems were encountered in extrapolating the reflectivity measurements above 22 eV for the Kramers-Kronig analysis due to the fact that interband

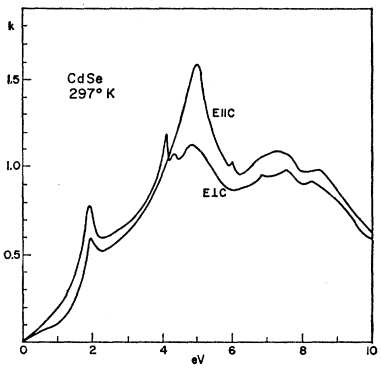

FIG. 12. Room-temperature absorption index of hexagonal CdSe for $E\perp c$ and $E\|c$.

transitions are still strong at this energy. With the standard $R\sim E^{-4}$, free-electron law, negative absorption coefficients were found at low energies. The exponent

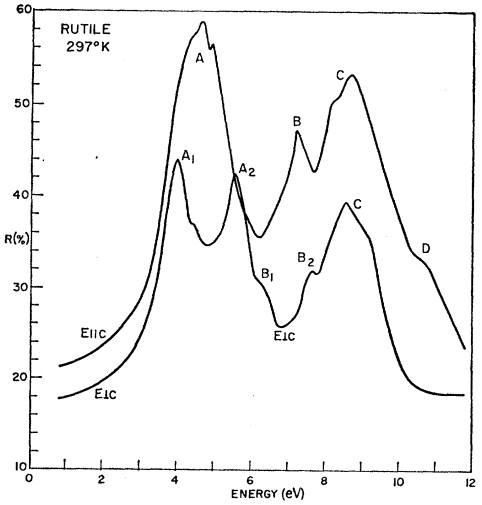

FIG. 13. Room-temperature reflectivity of rutile for $E\perp c$ and $E\|c$ between 1 and 12 eV.

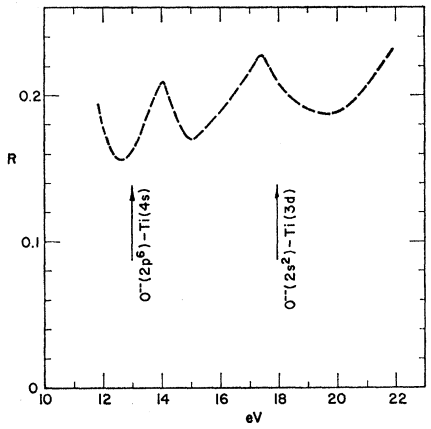

FIG. 14. Room-temperature reflectivity of rutile between 12 and 22 eV for unpolarized light.

of the energy was modified *ad hoc* until no negative absorption coefficients were obtained and a sharp A absorption edge resulted. Figures 15 to 17 show the wavelength dependence of the optical constants n, k and $\epsilon_2=2nk$ deduced from $R(E)$ by this Kramers-Kronig analysis.

IV. DISCUSSION

A. Wurtzite

The interpretation of the structure in the optical data of the wurtzite crystals has to be based on the existing knowledge of zincblende materials and the expected changes in the electronic structure from zincblende to wurtzite. On the basis of the existing knowledge of diamond- and zincblende-type materials arrived at by discussing the optical data with the help of pseudopotential band-structure calculations[23,24] and

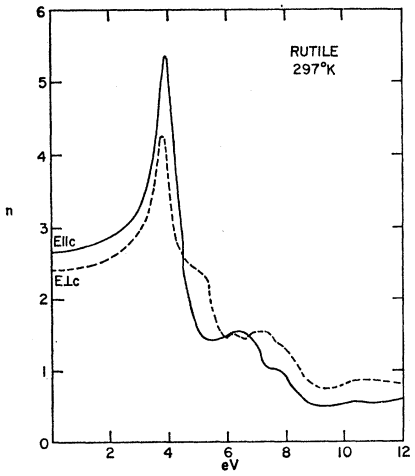

FIG. 15. Room-temperature refractive index of rutile for $E\perp c$ and $E\|c$.

[23] D. Brust, J. C. Phillips, and F. Bassani, Phys. Rev. Letters 9, 94 (1962).

[24] D. Brust, M. L. Cohen, and J. C. Phillips, Phys. Rev. Letters 9, 389 (1962).

TABLE II. Energies of the peaks in reflection (R), absorption index (k), and imaginary part of the dielectric constant (ϵ_2) observed in rutile at room temperature.

	$E\perp c$			$E\|c$		
	R	k	ϵ_2	R	k	ϵ_2
A	3.97 5.52	4.10 5.51	4.00 5.35	4.60	4.35	4.11
B	6.50 7.64	6.45 7.64	6.1 7.4	7.21	7.15	6.63
C	8.53 9.24	8.25 9.2	8.05	8.16 8.68	8.05 8.6	7.87
D	...	...	...	10.7		
	unpolarized					
E	14.1					
F	17.4					

the isoelectronic sequence scheme[7,5,10] one is able to predict the energies of reflectivity peaks in the hypothetical zincblende analogs of the wurtzite materials under consideration and to identify the peaks in the spectrum of cubic ZnS. The expected changes from zincblende to wurtzite can be discussed by comparing the Brillouin zones of both types. Figure 18 shows both Brillouin zones, the truncated octahedron of zincblende and the hexagonal prism of wurtzite. The number of atoms per wurtzite unit cell is twice that of zincblende and hence the Brillouin zone of wurtzite has one-half the volume of that of zincblende. In order to obtain approximate fit between both zones the wurtzite zone in Fig. 18 is doubled following the double zone scheme of Birman.[9] In this author's perturbation approach a correspondence is obtained between the [111] direction ΓL in zincblende and the c axis $\Gamma A\Gamma$ in wurtzite. However, this correspondence holds only for two of the eight equivalent ΓL directions of zincblende, namely the $\pm[111]$ directions. The electronic states along the other six directions ($\pm[\bar{1}11]$, $\pm[1\bar{1}1]$, $\pm[11\bar{1}]$ of zincblende) cannot be derived by this perturbation approach. The number of $\Gamma(\mathbf{k}=0)$ states in wurtzite is double that of zincblende. Half of the Γ wurtzite states correspond directly to Γ states of zincblende. The triplet states of zincblende (Γ_{15}) correspond to a doublet (Γ_5) and a singlet (Γ_1). The Γ_5-Γ_1 splitting of

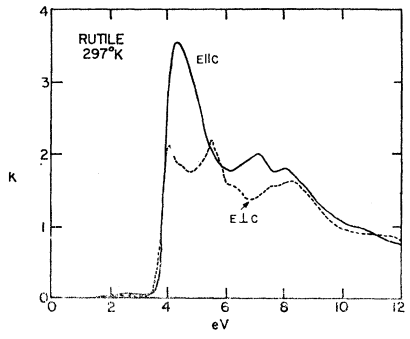

FIG. 16. Room-temperature absorption index of rutile for $E\perp c$ and $E\|c$.

the top valence band is obtained from the $E\|c$-$E\perp c$ splitting of the absorption edge[11–13] and is rather small ($\approx$0.03 eV). We believe that the splitting of other Γ_{15} states should be of the same order of magnitude. When spin effects are taken into account, the hexagonal crystal field introduces linear terms in $\mathbf{k}$ in all Γ_1 states. The effect of these terms, however, is believed to be rather small and beyond the resolution of the type of experiments described here.[25] Due to the folding of the double zone into the reduced zone, states appear at Γ in wurtzite which do not correspond to Γ states of zincblende. These states have Γ_6 and Γ_3 symmetry and correspond to L states of zincblende (Γ_3 corresponds to L_1 and Γ_6 to L_3). There is evidence that the optical matrix elements between Γ states of wurtzite which do correspond to zincblende and those which do not (such as $\langle\Gamma_6|p|\Gamma_5\rangle$) are rather small.[26]

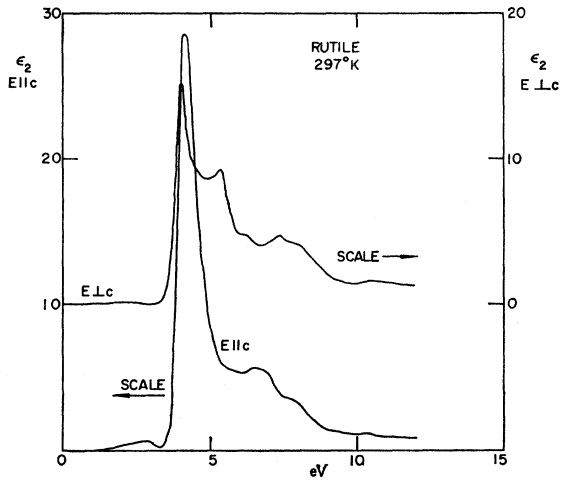

FIG. 17. Imaginary part of the dielectric constant of rutile for $E\perp c$ and $E\|c$.

Following the wurtzite-zincblende analogy, the E_0' peak of ZnS and the E_1 peaks in CdS were tentatively interpreted.[10,15,27]

The peak A in Fig. 4 and the A_1–A_2 doublet in Fig. 5 have been assigned[15] to Δ_5–Δ_1 or to Δ_6–Δ_3 transitions (Δ is a general point along the c axis) which are only allowed for $E\perp c$. Following the germanium-zincblende-wurtzite analogy this is a point at which $\nabla_k(E_c-E_v)=0$ but $\nabla_k E_c\neq 0$ (see Fig. 19). It is not possible to decide conclusively whether the transitions involved are Δ_5–Δ_1 or Δ_6–Δ_3, that is, in the double zone scheme, at what side of the midpoint of Γ–Γ' (A point) they occur. However, the fact that in germanium the Λ point at which the transitions causing E_1 take place is at a distance 0.18 ($\Gamma-L$) away from Γ, seems to indicate that the Δ_5–Δ_1 transitions are the likeliest to cause the

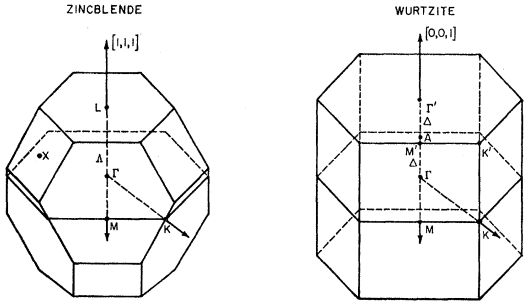

FIG. 18. Brillouin zone of zincblende and double Brillouin zone for the corresponding wurtzite-type material (from Ref. 27).

$E_1(A)$ structure of wurtzite. The A_1–A_2 doublet of CdSe is caused by the spin-orbit splitting of Δ_5. Such splitting is also seen[15] in CdS at 4°K. We prefer this identification of the A structure to that of Phillips[27] (K_3–K_2 transitions). The K_3–K_2 transitions have no high-symmetry zincblende analog and hence Phillips' interpretation was based on a preliminary band calculation for hexagonal ZnS.[28] The inaccuracy of such calculations, due among other things to the difficulties in estimating core shifts, is well known. The calculations

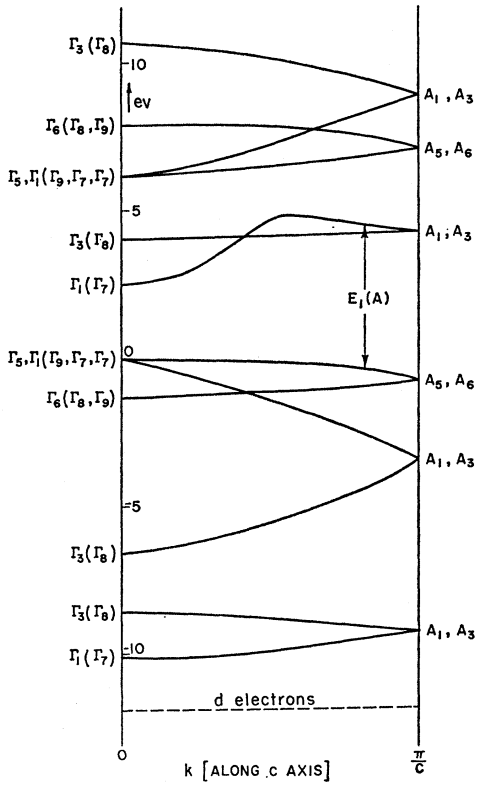

FIG. 19. Band structure of CdS along the hexagonal axis. The double group representations at Γ are given in brackets.

[25] G. D. Mahan and J. J. Hopfield, Phys. Rev. **135**, A428 (1964).
[26] M. Cardona, Phys. Chem. Solids **24**, 1543 (1963).
[27] J. C. Phillips, Phys. Rev. **133**, A452 (1964).
[28] F. Herman and S. Skillman, in *Proceedings of the International Conference on Semiconductors, Prague 1960* (Czechoslovakian Academy of Sciences, Prague, 1961), p. 20.

in Ref. 28 yield, for instance, the wrong order for the Γ_5, Γ_1, and Γ_6 highest valence band states.

Phillips also attributes weak structure observed near A_1 and A_2 for $E\|c$ to transitions at $H(H_3-H_3)$. This structure could, however, be due to the same transitions causing A_1 and A_2, forbidden for $E\|c$, and a slight sample misalignment. The origin of the B peaks of wurtzite, supposedly the analog of the $\pm[\bar{1}11]$, $\pm[1\bar{1}1]$, $\pm[11\bar{1}]$ contributions to the E_1 peak of zincblende is still uncertain. Phillips has proposed transitions at M for $E\perp c$ and at K for $E\|c$. At this point we should mention that there is some confusion in the literature about the notation of the irreducible representations at M. There are four irreducible representations M_1, M_2, M_3, M_4 in the usual Koster notation[29,30,9] equivalent to M_1, M_4, M_2, M_3, respectively, in the notation of Glasser,[31] used by Phillips,[27] and equivalent to M_1, M_4, M_3, M_2, respectively, in the notation of Rashba,[32] used by Herman.[28] From the selection rules[33] it can be seen that there exist four possible transitions for $E\|c$ between states at M: M_1–M_1, M_2–M_2, M_3–M_3, and M_4–M_4, and four transitions for $E\perp c$, namely M_1–M_3, M_1–M_4, M_2–M_3, M_2–M_4 in the Koster notation. However, there is at present not enough knowledge about the states at M to give any assignment. Not even the correspondence between the six $\pm[\bar{1}11]$, $\pm[1\bar{1}1]$, $\pm[11\bar{1}]$ directions and the Γ-M direction is unambiguously established. It could equally well be the direction Γ-P (labeled Σ) which offers the possible transitions Σ_1–Σ_1 for $E\|c$ and $E\perp c$ and Σ_1–Σ_2 for $E\perp c$. In spite of this uncertainty in the assignment of the E_1 transitions, which will be resolved with more detailed band calculations for wurtzite, the different polarization effects on the first strong-reflection maxima in ZnS (E_0') on one side, and CdS and CdSe (E_1) on the other side, are very conclusive as to the type of transitions causing the maxima. As mentioned in III the ZnS spectrum is of the silicon type with the E_0' peak dominating the E_1 peak in contrast to the germanium type. The transition between both types of reflection spectra can be illustrated for the Ge-Si alloys. As discussed by Bassani and Brust,[34] the $\Gamma_{2'}$ conduction band minimum in germanium moves rapidly to higher energies when silicon is added to the material. L_1, somewhat less s-like, moves less than $\Gamma_{2'}$, while $\Gamma_{25'}$, $L_{3'}$, and L_3 move little with alloying. Hence the position of the Λ_3–Λ_1 (E_1) saddle point is shifted towards Γ with increasing silicon content. This produces a decrease in the strength of the E_1 peak (see also the CuCl-CuBr system[21]) as it moves to coincide with E_0' with increasing silicon concentration. As $\Gamma_{2'}$ crosses Γ_{15}, L_1 becomes connected with Γ_{15} and the saddle point disappears. In GaP and CuCl, Γ_1 (equivalent to $\Gamma_{2'}$ of germanium) is still below Γ_{15}, but the E_1 peak has become so weak that the lowest energy reflection peak is mainly E_0' (Γ_{15}–Γ_{15}). The small temperature[35] and pressure[20] coefficients of the lowest reflection peak in GaP confirm its predominantly E_0' (Γ_{15}–Γ_{15}) nature although weaker E_1-type transitions occur at about the same energy.

In ZnS again the Γ_1 conduction band is lower than the Γ_1, Γ_5 conduction bands (Γ_{15} in zincblende) and one expects also such a composite peak. The fact that polarization effects are almost completely absent in our measurements, in contrast to CdS and CdSe, demonstrates that there is only a small admixture of Λ or Δ transitions in this peak. Γ transitions are almost unaffected by the transformation from zincblende to wurtzite, as expected since there is little interaction between the Γ_6 and Γ_3 states added to the Γ_5 and Γ_1 states already present at Γ. This also explains the small polarization effects at the absorption edge.[11,12,13] E_1 may be causing the shoulder seen just below E_0' in Fig. 3.

The E_1' peak in zincblende is due to L_3–L_3 transitions. The perturbation scheme brings one of the four equivalent L points into Γ and the corresponding Γ_6–Γ_6 transitions are only allowed for $E\|c$. The other three L points go to points of lower symmetry than Γ, where transitions for both polarizations are probably allowed. Thus one should expect a doublet for $E\|c$ and a single peak for $E\perp c$. The doublet is unresolved in our measurements, but in all three materials the position of E_1' is between 0.12 and 0.28 eV higher for $E\|c$ than for $E\perp c$. This result is in accordance with the predictions and shows that the Γ_6–Γ_6 transitions are at higher energy than those at the points of lower symmetry.

The F_1 peak, which is not observed in zincblende, shows up for $E\perp c$ and has its position in all three materials at 0.4 to 0.8 eV lower energies than the E_2 peak. This might be associated with the fact that the [100] direction in zincblende does not fall on any high symmetry direction of wurtzite but we cannot give any definite assignment for F_1.

The d_1 peaks appearing in all three materials at nearly the same energy (11 eV) as in ZnTe, CdTe, HgTe,[5] HgSe,[36] and GaP,[4] have been attributed in zincblende to L_3–L_1 transition.[27] There seem to be small polarization effects on the corresponding peaks in wurtzite due to Γ_6–Γ_3 transitions, allowed for $E\perp c$ and other transitions allowed for both oritentations. Also the F_3 shoulder in CdS and CdSe exhibits a small difference for $E\perp c$ and $E\|c$. d-electron transitions[5] are seen in our measurements in the form of the broad d_2 peak in Fig. 3.

Figure 19 shows the band structure of CdS along the

[29] G. F. Koster, *Solid State Physics*, edited by F. Seitz and D. Turnbull (Academic Press Inc., New York, 1957), Vol. 5, p. 174.
[30] R. C. Casella, Phys. Rev. **114**, 1514 (1959).
[31] M. L. Glasser, Phys. Chem. Solids **10**, 229 (1959).
[32] E. I. Rashba, Fiz. Tverd. Tela **1**, 407 (1959) [English transl.: Soviet Phys.—Solid State **1**, 368 (1959)].
[33] F. Bassani (private communication).
[34] F. Bassani and D. Brust, Phys. Rev. **131**, 1524 (1963).
[35] M. Cardona, J. Appl. Phys. **32**, 2151 (1961).
[36] W. J. Scouler and G. B. Wright, Phys. Rev. **133**, A736 (1964).

TABLE III. Reflection peaks observed in diamond-, zincblende- and wurtzite-type materials, selection rules, and points in **k** space at which the transitions seem to occur.

	Diamond	Zincblende	Wurtzite $E\|\|c$	Wurtzite $E\perp c$
E_0	$\Gamma_{25'}\rightarrow\Gamma_{2'}$	$\Gamma_{15}\rightarrow\Gamma_1$	$\Gamma_1\rightarrow\Gamma_1$	$\left.\begin{matrix}\Gamma_5\\ \Gamma_1\end{matrix}\right\}\rightarrow\Gamma_1$
E_0'	$\Gamma_{25'}\rightarrow\Gamma_{15}$	$\Gamma_{15}\rightarrow\Gamma_{15}$	$\Gamma_5\rightarrow\Gamma_5$ $\Gamma_1\rightarrow\Gamma_1$	$\Gamma_5\rightarrow\Gamma_1$ $\Gamma_1\rightarrow\Gamma_5$
E_1 $\begin{matrix}A\\B\end{matrix}$	$\Lambda_3\rightarrow\Lambda_1$	$\Lambda_3\rightarrow\Lambda_1$	forbidden $M_1\rightarrow M_1$, $K_2\rightarrow K_2$, $\Sigma_1\rightarrow\Sigma_1$	$\Delta_5\rightarrow\Delta_1$ $M_2\rightarrow M_4$, $M_1\rightarrow M_4$, $\Sigma_1\rightarrow\Sigma_2$
E_1'	$L_{3'}\rightarrow L_3$	$L_3\rightarrow L_3$	$\Gamma_6\rightarrow\Gamma_6$ and others	unknown
E_2	$X_4\rightarrow X_1$	$X_5\rightarrow\left\{\begin{matrix}X_4\\X_3\end{matrix}\right.$	unknown	unknown
d_1	$L_{3'}\rightarrow L_{2'}$, (forbidden)	$L_3\rightarrow L_1$	unknown	$\Gamma_6\rightarrow\Gamma_3$ and others
d_2	from d electrons	from d electrons	from d electrons	from d electrons
F_1	...	...	forbidden	unknown
F_2	...	unknown	...	...
F_3	...	...	unknown	unknown

c axis, as obtained from our measurements and other work. Table III lists the reflection peaks observed in zincblende and wurtzite, their relationship, and the corresponding selection rules.

Walker and Osantowski[37] recently reported reflectivity measurements on CdS with unpolarized light. They observed a doublet at 9.3–9.7 eV (E_1' peak), which they attributed to transitions from the Γ_5 valence band to the second lowest Γ_1 conduction band, split from a Γ_5 conduction band by the hexagonal crystal field. As discussed above, we believe these transitions to be responsible for E_0' instead. The spin-orbit splitting of the Γ_5 valence band (0.06 eV) is far too small to account for the 9.3–9.7 eV doublet, as proposed by Walker and Osantowski. Walker[38] has also reported reflectivity measurements on CdS with polarized light. The position of his observed peaks agrees quantitatively with the peaks reported here. His 9.2–9.6 doublet (our E_1') is well resolved while it does not appear to be resolved in our measurements.

The F_1 peak at 7.0–7.1 eV is believed by Walker to be the same as the 6.3 eV peak of CdSe. As shown in Table I this is not the case. The F_1 peak occurs in CdSe at 6.2 eV. We believe the 6.3 eV peak of CdSe is E_0', which occurs in CdS at 6.1 eV.

Balkanski and Petroff[39] have studied the normal incidence reflection spectra of cubic ZnS and wurtzite-type ZnS, CdS, and CdSe with unpolarized light. The direction of propagation of the incident light was either parallel or perpendicular to the c axis. The results with the light propagating to the c axis parallel orientation ($E\|c$) agree very well with our data. When the light is propagated perpendicular to the c axis, both orientations $E\|c$ and $E\perp c$ are mixed (not equally since the instrument grating partially polarizes the light) and consequently the peaks observed are a mixture of the $E\|c$ and $E\perp c$ peaks.

Spicer and Kindig[40] measured the kinetic-energy distribution of the photoemitted electrons in CdS as a function of photon energy of the incident light. They see two types of peaks in the energy-distribution curves. For the one type, the position of the peak does not change when the photon energy is varied; hence these peaks are interpreted as due to a maximum in the density of states of the conduction band. The other type of peaks shift in energy by an amount equal to the shift in the energy of the incident photon; these peaks are interpreted as due to maxima in the density of states of the valence band. These authors conclude that the existence of the two types of peaks is evidence of the nonconservation of **k** in the light absorption process. The consistency of our interpretation of the optical properties of CdS and other wurtzite-, diamond-, and zincblende-type materials as due mainly to **k**-conserving processes speaks against Spicer and Kindig's interpretation. In particular, the strong polarization effects reported for wurtzite-type materials require **k** conservation. Direct evidence for at least partial **k** conservation in the photoemission process has also been recently presented.[41] We believe that it is possible to explain the peaks which do not shift with photon energy as due to **k**-conserving optical transitions. The excited electrons are scattered down to states of lower energy before emission takes place. For a scattering time

[37] W. C. Walker and J. Osantowski, Phys. Chem. Solids **25**, 778 (1964).

[38] W. C. Walker, Phys. Rev. Letters **13**, 51 (1964).

[39] M. Balkanski and Y. Petroff, in *Proceedings of the International Conference on Semiconductors, Paris 1964* (to be published). We wish to thank the authors for a communication of their results prior to publication.

[40] W. E. Spicer and N. B. Kindig, Solid State Commun. **2**, 13 (1964).

[41] G. W. Gobeli, F. G. Allen, and E. O. Kane, Phys. Rev. Letters **12**, 94 (1964).

inversely proportional to the density of states, a rather likely situation, most of the emission peaks will occur from conduction-band extrema and hence the peaks will not shift with photon energy. Hence the peaks in the energy distribution at 0.6 and 1.8 eV would correspond to conduction band extrema 0.6 or 1.8 eV+4.0 eV (electron affinity) +2.4 eV (energy gap)=7.0 or 8.2 eV above the top of the valence band. The 7.0-eV peak could be related to E_2 or to F_1. The 8.2-eV peak is most likely due to the conduction-band minimum involved in E_1'. The position of this minimum with respect to the top of the valence band can be estimated from the standard Γ_5–Γ_6 separation, approximately equal to 1.2 eV (it should be about equal to the Γ_{15}–L_3 separation of zincblende[6]). This minimum should thus be $E_1'-1.2=8$ eV above the top of the valence band, in agreement with our interpretation of the peak in the velocity distribution. The peak in energy distribution which shifts the full shift in photon energy must be due, as suggested in previous work,[40] to a flat valence band, possibly Γ_6 since this band is about 1 eV below Γ_5, Γ_1.

B. Rutile

The energy-band structure of the hexagonal wurtzite materials discussed so far can be described as that of a slightly perturbed cubic crystal. This is no longer true for rutile, although the relative atomic arrangement between titanium and oxygen in rutile is similar to that of cubic $SrTiO_3$ and $BaTiO_3$ and, as a consequence, the first absorption edges in rutile[18], $SrTiO_3$,[42] and $BaTiO_3$,[43] presumably due to transitions between oxygen-like and titanium-like wave functions, all occur at about the same energy. The strong polarization effects at higher energies, shown in Fig. 13, give evidence for different behavior of the higher transitions. The optical constants, as determined from our measurements, explain the long-wavelength birefringence and dispersion of rutile. The low-energy end of the refractive-index curves in Fig. 15 is in agreement with the measurements of Devore.[17] Devore fitted his results between 4350 and 15 000 Å with the formula

$$n^2=a+b/(\lambda^2-\lambda_0^2),$$

that is, with a single-harmonic-oscillator model, with $\lambda_0=2830$ Å (equivalent to 4.38 eV) for $E\perp c$ and $\lambda_0=2905$ Å (equivalent to 4.27 eV) for $E\|c$. The imaginary part of the refractive index in Fig. 16 does exhibit one dominating absorption band for $E\|c$ centered at 4.3 eV in excellent agreement with the refractive index data. For $E\perp c$ one has two absorption bands which mainly determine n at long wavelengths. The center of both bands combined additively is about 0.2 eV higher than the peak position for $E\|c$, in good agreement with Devore's one-oscillator fit of $n_\perp(\lambda)$. The dispersion and birefringence of rutile is thus determined by the energy region of highest absorption constant ($\alpha\sim1.5\times10^6$ cm^{-1} for $E\|c$ and $\alpha\sim1\times10^6$ cm^{-1} for $E\perp c$) and not by the first absorption edge.[17]

The imaginary part of the dielectric constant in Fig. 17 is a measure of the joint density of conduction and valence-band states as a function of energy, since the oscillator strength is, presumably, a slowly varying function of energy. We notice the dominating peak around 4–5 eV, particularly for $E\|c$. This behavior has not been encountered so far in other materials of the diamond-zincblende-wurtzite family. It indicates rather flat conduction and valence bands, running nearly parallel, or strong exciton effects. Both of these effects are expected for a strongly ionic crystal like rutile.

The energy bands of strongly ionic crystals can be calculated with reasonable accuracy with the LCAO (linear combination of atomic orbitals) method. This was done for cubic $SrTiO_3$ by Kahn and Leyendecker[44] who obtained very flat bands along the [100] direction. Preliminary calculations for rutile[44] show much similarity to $SrTiO_3$, resulting from the fact that the electronic structure is dominated by the octahedral configuration of the six oxygen ions surrounding the titanium. Nevertheless, if we accept that the valence band wave functions are derived mainly from oxygen $2p$ orbitals and the conduction-band wave functions primarily from $3d$ orbitals of titanium and that the fundamental edge corresponds to transitions between these states, we have to conclude that the structure up to 10 eV arises from band-structure (and possibly exciton) effects in those two sets of bands. The first ionic transition at higher energy different from $O^{2-}(2p^6)$-$Ti^{3+}(3d)$ is to be expected within the O^{2-} ion, namely $2p$–$3s$, at 10.7 eV.[45] In this energy region we observe the D-band (see Fig. 13). (The transitions within the O^{2-} ion have been derived from the atomic spectra of neutral Ne.) The transitions $O^2(2p^6)$-Ti$(4s)$ and $O^{2-}(2s^2)$–Ti$(3d)$ are indicated in Fig. 14 based on the value of 3 eV for $O^{2-}(2p^6)$–Ti$(3d)$.

ACKNOWLEDGMENTS

We would like to thank O. Tkal for assistance in the measurements and G. Neighbor and R. T. Smith for orienting the samples. We also want to thank Dr. L. Grabner for supplying the cleaved rutile samples.

[42] J. A. Noland, Phys. Rev. **94**, 724 (1954).
[43] R. C. Casella and S. P. Keller, Phys. Rev. **116**, 1469 (1959).
[44] A. H. Kahn and A. J. Leyendecker, in *Proceedings of the International Conference on Semiconductors, Paris 1964* (to be published).
[45] C. E. Moore, Natl. Bur. Std., U. S., Circ. 467 Vol. I (1949) and Vol. II (1952).